Advances in Bioresearch
Adv. Biores., Vol 17 (6) June 2026: 78-86

Print ISSN 0976-4585; Online ISSN 2277-1573
Journal's URL:http://www.soeagra.com/abr.html
CODEN: ABRDC3
DOI: 10.15515/abr.0976-4585.17.6.7886

Advances in Bioresearch

ORIGINAL ARTICLE

Green-Synthesised Chitosan–Iron Oxide Nanocomposites as Potent Anticancer Agent: Apoptotic and Mechanistic Insights

Santhosh Abhirami and Pawlin Vasanthi Joseph*
Department of Zoology, Nirmala College for Women, Coimbatore, Tamil Nadu 641018, India.
***Correspondence Author:** Pawlin Vasanthi Joseph
Email: pawl_06@rediffmail.com

ABSTRACT
The Chitosan-Reduced Magnetic Iron Oxide nanocomposite (Cs-RMIO) was tested for its anticancer effects on HepG2 liver cancer cells. The previously characterised nanomaterial was evaluated using in vitro cytotoxicity and mechanistic studies. Cs-RMIO nanocomposite showed a significant, dose-dependent decrease in cell viability, along with increased cell death and morphological changes. Mechanistic investigations revealed that the Cs-RMIO nanocomposite generated Reactive Oxygen Species within cells, leading to oxidative damage. Fluorescence imaging confirmed substantial loss of cell viability and mitochondrial dysfunction. DAPI staining clearly showed chromatin condensation and DNA fragmentation, signs of apoptosis. Biochemical assays indicated increased lipid peroxidation and lactate dehydrogenase (LDH) release, along with alterations in antioxidant enzymes, including superoxide dismutase (SOD) and catalase, suggesting a disrupted redox balance. The apoptosis process was further confirmed by elevated caspase-9 and caspase-3 activity, demonstrating activation of the mitochondrial apoptotic pathway. Overall, these results suggest that Cs-RMIO nanocomposites have a strong anticancer effect through a combination of oxidative stress induction and apoptosis. The study highlights the potential of the Cs-RMIO nanocomposite as a capable nanotherapeutic for liver cancer, and calls for further research in advanced biological models.
Keywords: *Cs-RMIO NC, HepG2 liver cancer cells, Apoptotic pathway, Oxidative stress, Nanotherapeutic*

Received 04.04.2026 Revised 11.05.2026 Accepted 30.05.2026

How to cite this article:
Santhosh A and Pawlin Vasanthi J. Green-Synthesised Chitosan–Iron Oxide Nanocomposites as Potent Anticancer Agent: Apoptotic and Mechanistic Insights. Adv. Biores. Vol 17 [6] June 2026. 78-86

INTRODUCTION

Cancer continues to be one of the top causes of death globally, highlighting the need for more effective treatment strategies [1]. Conventional cancer treatments such as surgery, chemotherapy, and radiation can cause nonspecific adverse effects. Nanoparticle-based tailored drug delivery systems offer various benefits over traditional methods, including longer circulation time, controlled drug release, increased cellular uptake, lower systemic toxicity, and improved treatment effectiveness, while minimising tissue damage [2]. The application of green nanotechnology has accelerated the development of nanocarriers by emphasising environmentally friendly and biocompatible production methods. Chitosan is among the most prominent natural polymers for functionalizing nanoparticles. It is a natural, hydrophilic, and cationic polymer containing primary amine and hydroxyl groups, which can be used to modify nanoparticles [3]. The desirable biological features of chitosan, such as low immunogenicity, biocompatibility, high biodegradability, and minimal toxicity, further support its suitability for biomedical applications [4]. However, conventional chitosan extraction is limited by the use of toxic agents, which present environmental concerns. As an alternative, natural deep eutectic solvents (NADES) have emerged as greener extraction methods to mitigate the need for harmful reagents and progress sustainability. Chitosan, in particular, enhances the biological performance of nanomaterials and also acts as a reducing and stabilising agent in the eco-friendly synthesis of various nanoparticles [5]. Several studies have demonstrated that chitosan has been used to reduce and stabilise gold nanoparticles [6], silver nanoparticles [7], copper nanoparticles [8], and an iron oxide nanoparticle [5] during the green production process. In this regard, magnetic iron oxide nanoparticles have emerged as a unique class of

nanoparticles with tremendous potential for therapeutic and diagnostic applications, particularly in cancer treatment [9, 10]. Among various nanomaterials, metallic oxide nanoparticles have shown promising results, and their biomedical potential has been further enhanced through surface modification with biopolymers such as chitosan, thereby improving their biocompatibility and biological properties [11]. Iron oxide nanoparticles stand out because of their unique physicochemical and magnetic properties. It is particularly desirable in medical research owing to its inherent stability, biocompatibility, and ability to cross biological barriers [12]. Fe_3O_4 (magnetite) nanoparticles are preferred over other forms of iron oxide, including goethite, wustite, maghemite, and hematite, due to their low toxicity and high biocompatibility. injectability, chemical stability, saturation, and magnetic properties, superparamagnetic property, interaction with biomolecule dispersions, and simple synthesis[13]. In our previous publication [5] We described the preparation, characterisation, and biological applications of chitosan-reduced iron oxide nanocomposite (Cs-RMIO NC)[5]. Relaying on previous findings, this research investigates the anticancer activity of the material to evaluate its potential as a nanotherapeutic option for treating HepG2 cancer cells. Thus, the study was conducted to systematically assess their cytotoxic and mechanistic impacts on HepG2 cancer cells. A series of in vitro assays, including cell viability, ROS measurement, Mitochondrial Membrane Potential, DNA damage, biochemical enzyme analysis, and caspase activity, was performed to elucidate the fundamental apoptotic pathways.

MATERIAL AND METHODS

Synthesis and characterisation of Cs-RMIO nanocomposite

In our prior research, the Cs-RMIO nanocomposite was synthesised and characterised using XRD, FT-IR, SEM, TEM, FE-SEM, and ZETA DLS [5]. These findings confirmed the successful production of crab chitosan through NADES and the reduction of magnetic chitosan using crab chitosan itself, leading to the development of the Cs-RMIO nanocomposite with suitable size, shape, and functional properties. Building on these results, the current study investigates the anticancer activities of the previously identified nanocomposite.

Culturing and maintenance of cells:

Human lung carcinoma cancer cells (HepG2) were preserved in Dulbecco's Modified Eagle Medium (DMEM) enriched with 10% fetal bovine serum (FBS) and 1% penicillin-streptomycin, and incubated at 37°C in a humidified atmosphere containing 5% CO_2. Cells from exponentially expanding cultures were employed in further experiments [14].

Cytotoxicity and Morphological Evaluation in HepG2 cell lines

The cytotoxic potential of Cs-RMIO NC against HepG2 cell lines was assessed using both the MTT assay and microscopic evaluation of cellular morphology. For cytotoxicity studies, cells were seeded into 96-well plates at a density of 1×10^4 cells per well and allowed to adhere for 24 hours before treatment. Subsequently, they were exposed to varying concentrations of Cs-RMIO NC (3, 6, 12, and 24 µg/mL) for 24 hours, with untreated cells serving as the control. Following post-treatment, 20 µL of MTT solution (5mg/mL in PBS) was added to each well and incubated for 4 hours at 37°C. The formazan formed was dissolved in 150 µL of dimethyl sulfoxide (DMSO), and absorbance was measured at 570nm using a microplate reader. Cell viability was reported as a percentage compared to the untreated control. [15].

Evaluation of Reactive Oxygen Species (ROS)

Intracellular ROS levels in HepG2 cell lines were measured using the DCFH-DA assay. Cells were cultured in DMEM containing 10% FBS and 1% penicillin-streptomycin, then seeded into 6-well plates at 1×10^5 cells per well. After a 24-hour incubation, cells were exposed to Cs-RMIO NC (3, 6, 12, and 24 µg/mL) for an additional 24 hours, with untreated cells serving as controls. After treatment, the cells were washed twice with PBS and then incubated with 10 µM DCFH-DA in serum-free medium for 30 minutes at 37°C. Following PBS washes to remove residual dye, fluorescence intensity was measured at 485 nm (excitation) and 535 nm (emission). Morphological changes related to ROS production were observed using a fluorescence microscope. All experiments were conducted in triplicate. [16, 17].

Live/Dead Cell Imaging Assay-Dual staining method

Cell viability and apoptosis in HepG2 cells following exposure to Cs-RMIO NC were assessed through dual staining with Acridine Orange (AO) and Ethidium bromide (EB). Cells were seeded in 6-well plates (1×10^5 cells/well), incubated for 24 hours, then treated with (3,6,12, and 24 µg/mL) Cs-RMIO NC for 24 hours; untreated cells served as a control. Following treatment, cells were washed twice with PBS and stained with AO and EB (each at 100 µg/mL) for 5 min at room temperature in the dark. Stained cells were promptly visualised under a fluorescent microscope, with live cells fluorescing green (AO uptake) and apoptotic or dead cells appearing orange to red (EB uptake). Images were captured for morphological assessment, and all the tests were performed in triplicate [18].

Mitochondrial membrane potential Analysis (MMP)

Mitochondrial membrane potential in HepG2 cell lines exposed to Cs-RMIO NC was assessed using JC-1fluorescent dye. Cells were plated in 6-well plates at 1 × 10^5 cells per well and incubated for 24 hours to allow adherence. The cells were exposed to Cs-RMIO NC at concentrations of 3, 6, 12, and 24 µg/mL for 24 hours, with untreated cells as controls. Afterwards, they were rinsed twice with PBS and stained with 5 µM JC-1 in serum-free medium at 37°C for 20 minutes in the dark. Excess dyes were rinsed with PBS, and fluorescence was promptly noticed using a microscope. Healthy cells with intact mitochondria showed red fluorescence due to JC-1 aggregation, while cells with depolarised mitochondria exhibited green fluorescence from JC-1 monomers. Images were taken for morphological examination, and experiments were carried out in triplicate [19].

Assessment of DNA damage via DAPI staining

The evaluation of DNA damage in HepG2 cell lines subjected to Cs-RMIO NC was conducted using 4', 6-diamidino-2-phenylindole (DAPI) staining methodology. Cells (1 x 10^5 per well) were seeded in 6-well plates and allowed to attach for 24 hours. Subsequently, the cells were exposed to Cs-RMIO NC at concentrations of 3, 6, 12, and 24 µg/mL for 24 hours, with untreated cells as controls. After treatment, the cells were washed twice with phosphate-buffered saline (PBS) and fixed using 4% paraformaldehyde for 15 minutes. Following fixation, the cells were rinsed once more with PBS and stained with 1 µg/mL DAPI for 10 minutes in the dark. Excess dye was neutralised by washing with PBS, and nuclear morphology was examined using a fluorescence microscope with a UV filter. Damages or apoptotic nuclei were identified by chromatin condensation, fragmentation, or increased fluorescence relative to controls. Representative images were obtained for qualitative and quantitative evaluation [20].

Biochemical Assays (SOD, MDA, LDH, Catalase)

HepG2 cell lines (1 x 10^5 cells /well density) were cultured in 6-well plates and exposed to Cs-RMIO NC at a concentration ranging from 3,6,12, and 24 µg/mL for 24 hours. Untreated cells served as the control. After exposure, cells were rinsed with ice-cold PBS and lysed in RIPA buffer containing protease inhibitors. Lysates were centrifuged at 12,000 for 10 minutes at 4°C, and the supernatants were collected. Protein levels were measured using the Bradford assay. Superoxide dismutase (SOD) activity was assessed with a kit that measures inhibition of nitroblue tetrazolium reduction, with absorbance read at 560 nm. Lipid peroxidation was evaluated using the TBARS assay, which detects malondialdehyde (MDA) at 532 nm. Lactate dehydrogenase (LDH) activity in culture supernatants was analysed colourimetrically at 490 nm and expressed as percentage release relative to controls. Catalase activity was measured by monitoring hydrogen peroxide decomposition at 240 nm [11] [21].

Caspase-3 and Caspase-9 Activity Assays

The activities of caspase-3 and caspase-9 in HepG2 cell lines exposed to (Cs-RMIO NC) chitosan-reduced iron oxide nanocomposites 3,6,12, and 24 µg/mL for 24 hours were determined using a commercial colourimetric assay kit. The method relies on the cleavage of particular substrates, DEVD-pNA (caspase-3) and LEHD-pNA (caspase-9), which releases p-nitroaniline (*p*-NA). In each reaction, 50 µg of cell lysate protein was combined with 2× reaction buffer containing 10 mM dithiothreitol and 4 mM substrate in a final volume of 105 µL. Samples were incubated at 37°C for 1 hour, and absorbance was obtained at 405 nm. Caspase activity was measured as picomoles of pNA produced per minute per milligram of protein. [22].

Statistical analysis

All experimental results are expressed as mean ± SD. Statistical analysis was carried out using GraphPad Prism 8 (GraphPad Software, USA). Group differences were examined with one-way ANOVA, followed by Tukey's post hoc test for multiple comparisons. A p-value below 0.05 ($p < 0.05$) was considered statistically significant. Graphs and plots were generated directly within GraphPad Prism 8.

RESULT AND DISCUSSION

Cytotoxicity and Morphological Evaluation

The antiproliferative activity of the green-synthesised CS-RMIO nanocomposite was evaluated against HepG2 human cancer cells using the MTT assay over 48 hours at concentrations of 3, 6, 9, 12, and 24 µg/ml. The morphological changes in HepG2 cells after exposure to the nanocomposite were dose-dependent, as shown in Figure 1. The control cell exhibited normal polygonal morphology, intact cell membranes, and strong adherence to the culture surface. Results demonstrated that the nanocomposite exerted strong, dose-dependent cytotoxic effects, with the percentage of dead cells increasing significantly from 11.88% in the control to 78.88% at 12 µg/ml. Conversely, cell viability dropped sharply from approximately 96% in untreated cells to 24.8% at 24µg/ml. Live/dead dual staining visually confirmed these findings: control cells mainly exhibited green fluorescence, indicating viability, while

treated cells showed increasing red fluorescence, indicating cell death or membrane compromise. This inverse correlation between nanoparticle concentration and cell viability confirms the nanocomposite's antiproliferative effect. These results support prior research showing that chitosan-based metal nanomaterials improve cellular uptake and cytotoxicity due to their nanoscale size and surface properties, with chitosan-coated iron oxide nanoparticles showing even greater endocytosis and cytotoxicity at lower concentration doses[23]. Another study found that magnetically functionalized nanoparticles effectively killed tumour cells at doses as low as 10 µg/mL in vivo, confirming the efficiency of the Cs-RMIO nanocomposite in this investigation [24]. This increased activity may be due to chitosan's polycationic nature, which can disrupt negatively charged cell-surface residues and alter cell permeability, or to its ability to bind DNA, thereby inhibiting RNA synthesis [25, 26].

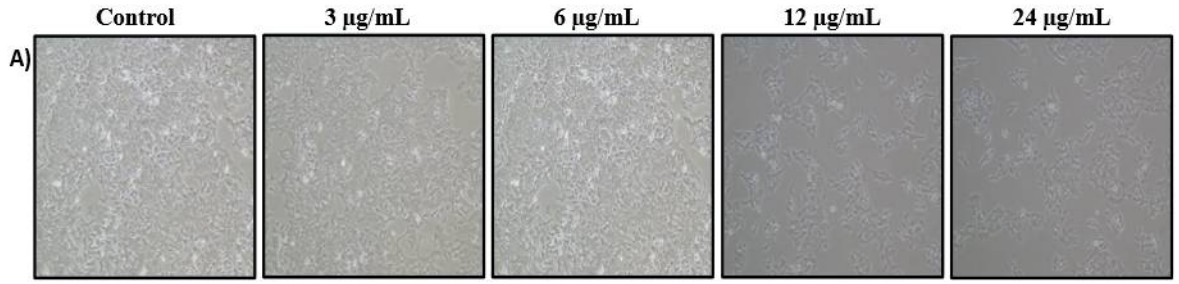

Figure.1: Representative microscopic images of HepG2 cells treated with Cs-RMIO NC were taken using an inverted phase contrast microscope. Control cells displayed normal morphology, while treated cells showed apoptotic changes that increased with the dose.

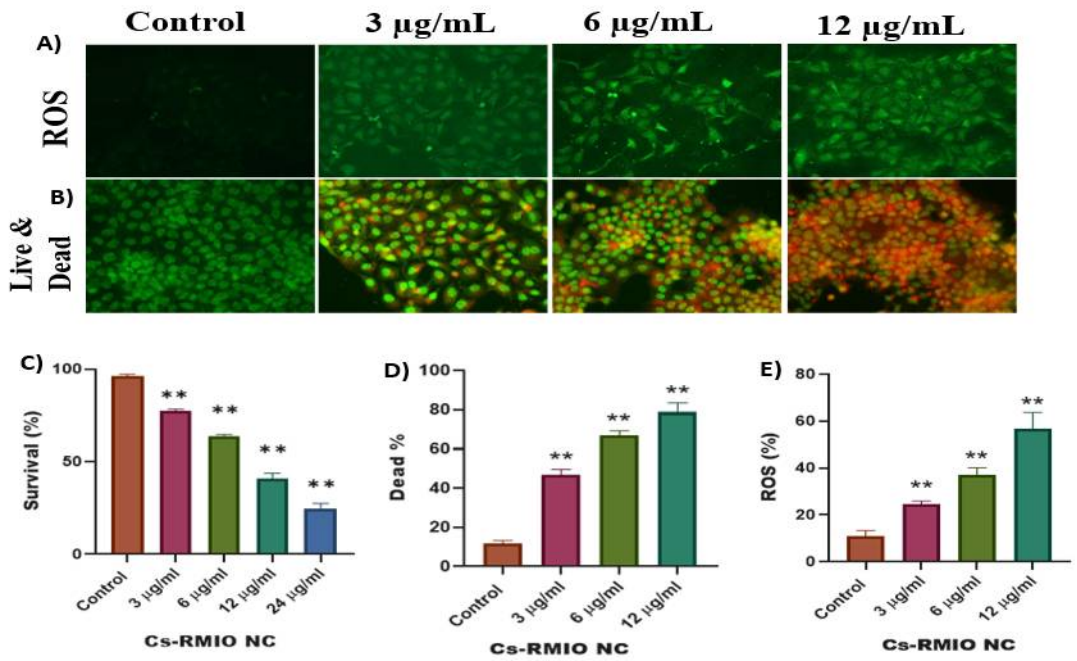

Figure. 2: Fluorescence images and quantitative analysis of (A) ROS generation and (B) Live/dead cell staining in HepG2 cells treated with Cs-RMIO NC at different concentrations. The corresponding graphs show decreases in cell viability, increases in cell death, and higher ROS levels, confirming oxidative stress-induced cytotoxicity.

Induction of Oxidative Stress and Membrane Damage

The cytotoxicity mechanism was clarified by analysing oxidative stress markers. Intracellular ROS levels, measured via DCFDA staining, showed a significant increase, with fluorescence intensity (RFU) rising from 10.8% in controls to 56.8% at the highest concentration. Fluorescence imaging confirmed this increase in ROS (Figure 2A); control HepG2 cells exhibited minimal fluorescence, while treated cells showed a notable increase in green fluorescence, which intensified with higher concentrations. This indicates substantial oxidative stress within the cells. Excessive ROS can damage key macromolecules,

such as lipids, proteins, and DNA, disrupting cellular balance[15]. In Cs-RMIO NC, the Chitosan improves stability and dispersibility and enhances cellular delivery. The iron oxide can catalyse Fenton-like reactions in which Fe^{2+}/Fe^{3+} ions react with cellular H_2O_2 to generate highly reactive hydroxyl radicals, thereby significantly increasing intracellular ROS[27]. Correspondingly, lipid peroxidation increased markedly, with MDA levels rising from 13.2% to 60.4%, suggesting severe membrane damage (Figure 3B). LDH release also increased from 13.2% in controls to 76.2% at 12 µg/mL, indicating membrane compromise and cell leakage (Figure 3A). The chitosan coating most certainly plays a subtle role in this process; the cationic amino groups of chitosan can interact electrostatically with the negatively charged phospholipid bilayer of cancer cells, enhancing direct membrane disruption in addition to ROS-mediated indirect damage [28, 29]. MDA is a byproduct generated during the peroxidation of polyunsaturated fatty acids caused by ROS, and it functions as a reliable biomarker of oxidative damage to cell membranes[30]. The elevated ROS, MDA, and LDH levels strongly imply that the Cs-RMIO nanocomposite induces oxidative stress-related cytotoxicity, a recognised pathway for nanoparticle-induced cancer cell death.

Modulation of Antioxidant Defence Systems

To assess increased oxidative stress, the activities of major antioxidant enzymes were measured. SOD activity increased significantly from 23.8% in control cells to 91.8% at 12µg/mL, while catalase activity decreased from 14.6% to 79.4% at the same concentrations, as shown in Figure 3D. The results showed a substantial, dose-related increase in SOD activity. According to Fahmy *et al.,* the SOD catalyses the dismutation of superoxide radicals (O2-) into hydrogen peroxide (H_2O_2) and oxygen. Increased SOD activity is an early cellular response to elevated ROS levels induced by nanoparticle-mediated oxidative stress. Excess superoxide radicals are converted to H_2O_2, which can damage cellular components and induce apoptosis [11]. The increased H_2O_2 activity indicates an initial cellular response. A decrease in catalase activity suggests oxidative damage, as lower CAT levels allow hydrogen peroxide to accumulate, intensifying oxidative stress and promoting apoptosis [31]. In Fe_3O_4-CS, ceria serves as a prooxidant in cancer cells, increasing SOD activity or mimicking it while decreasing the catalase activity. This causes an accumulation of H_2O_2, which is subsequently converted into highly delocalized hydroxyl radicals (●O2) via Fenton-type reactions, leading to severe oxidative stress and cancer cell death [32]. Fe_3O_4 nanoparticles, which magnetise the chitosan, produce ROS within cancer cells, causing oxidative stress that leads to cytotoxicity and programmed cell death. This imbalance results in cumulative oxidative damage, ultimately contributing to cell death.

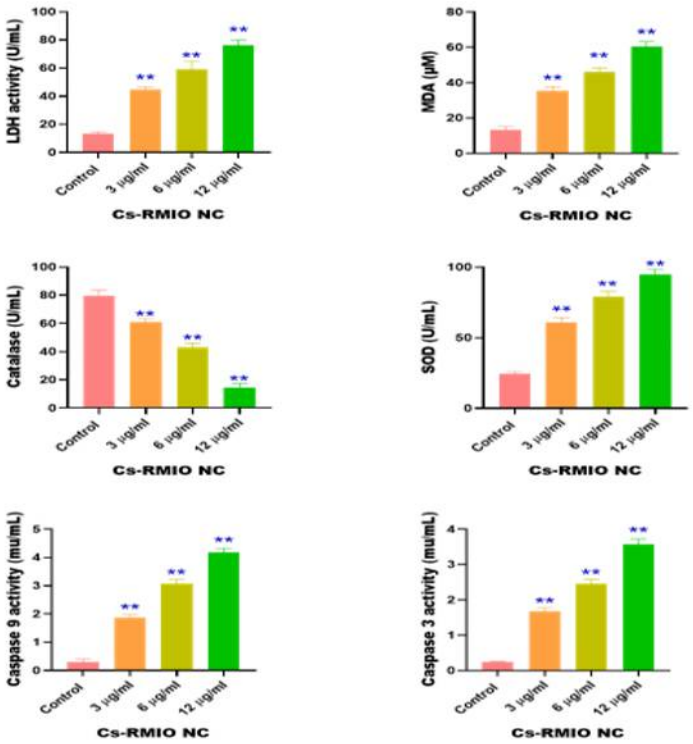

Figure 3: Biochemical assay results showing (A) Lactate dehydrogenase (LDH), (B) Malondialdehyde (MDA), (C) Superoxide dismutase (SOD), (D) Catalase, (E)Caspase 9, and (F) Caspase 3 activities in HepG2 cancer cells treated with varying concentrations of Cs-RMIO.

Mitochondrial Dysfunction and Loss of Membrane Potential

Mitochondrial membrane potential (MMP), a critical indicator of mitochondrial function, was significantly disrupted following treatment with Cs-RMIO nanocomposite. The observed increase in MMP disruption values, from 10.2% in control cells to 60.6% at 12 µg/mL, indicates significant mitochondrial depolarisation. Fluorescence imaging was employed to evaluate alterations in the mitochondrial membrane potential, as illustrated in Figure 4A. At higher concentrations, mitochondrial fluorescence decreased significantly, indicating severe mitochondrial dysfunction. Mitochondria are crucial for controlling apoptosis, and their dysfunction is often associated with the production of pro-apoptotic proteins. According to the literature, the observed loss of MMP in this study indicates that the Cs-RMIO nanocomposite induces mitochondrial instability, likely through Fe_3O_4 nanoparticle-induced ROS generation within cancer cells, thereby leading to oxidative stress [33]. This increase in ROS damages mitochondrial components, leading to MMP loss and the activation of apoptotic pathways [2]. Chitosan enhances the cellular uptake of Fe_3O_4, thereby promoting efficient ROS production in the mitochondria of cancer cells[25]. This combined effect enables the selective killing of cancer cells by impairing their mitochondrial function while sparing normal cells.

Assessment of DNA Damage via DAPI Staining

DNA damage and nuclear morphological alterations in HepG2 cells following treatment with the Cs-RMIO nanocomposite were evaluated using DAPI staining. In the control group, cells exhibited uniformly stained nuclei with intact, round morphology, indicating normal chromatin organisation and absence of nuclear damage. In contrast, cells treated with increasing concentrations of the Cs-RMIO nanocomposite exhibited pronounced nuclear abnormalities (Figure 4B). The qualitative observations from DAPI staining are consistent with the quantitative DNA damage data, which showed a substantial increase from 11.6% in control cells to 68% at higher concentrations. The induction of DNA damage is likely mediated by excessive Reactive Oxygen Species (ROS), which can cause oxidative modifications to DNA, leading to strand breaks and chromatin destabilisation [34]. According to earlier reports, iron oxide in the nanocomposite generates hydroxyl radicals (●OH) via the Fenton reaction, which attack the deoxyribose backbone of DNA, producing single- and double-strand breaks [11, 35, 36].

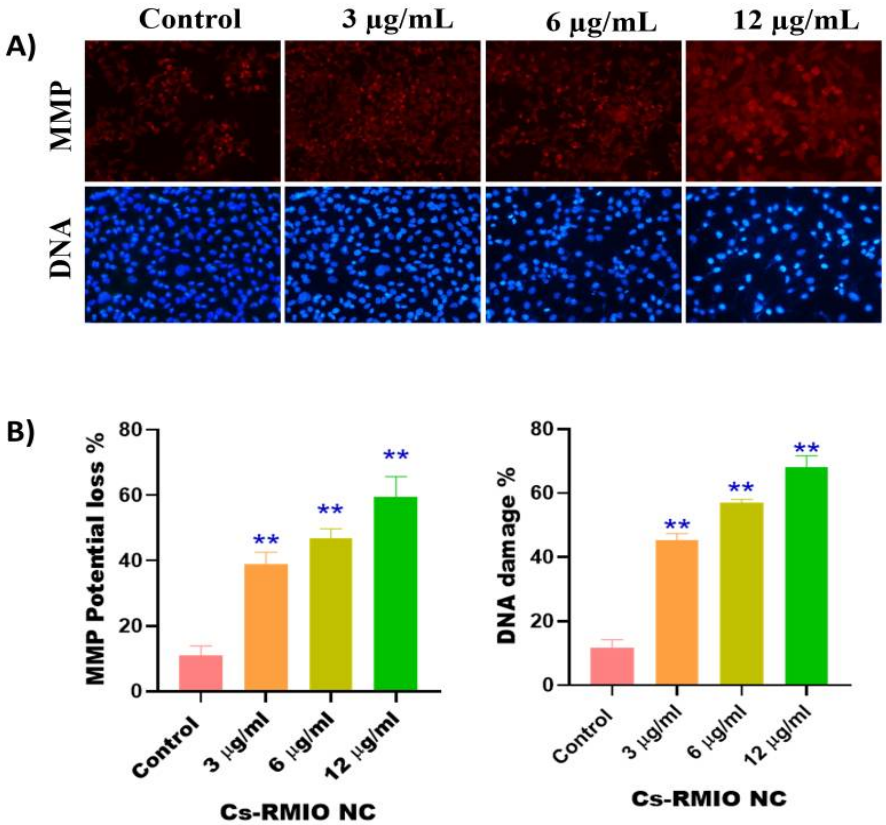

Figure 4: Fluorescence images showing (A) mitochondrial membrane potential (MMP) and DNA damage nuclear morphology (DAPI staining) in HepG2 cells treated with Cs-RMIO NC. (B) Quantitative graphs demonstrating (B) the percentage of MMP loss and (C) DNA damage in a dose-dependent manner, confirming apoptosis induction via the intrinsic pathway.

Activation of the apoptotic pathway

Apoptosis induction was verified by measuring caspase-9 and caspase-3 activities. Caspase-9 activity rose significantly from 0.3% in control cells to 4.16% at 12 μg/mL, while caspase-3 activity increased from 0.24% to 3.56% within the same concentration range (Figure 3E,3F). Caspase-9, an initiator caspase linked to the intrinsic (mitochondrial) apoptotic pathway, and caspase-3, an executioner caspase responsible for the final apoptotic stages, were both activated. Caspase-3 is a crucial molecule in the killing of cancer cells, and cleaved caspase -3 was found to be the primary enzyme responsible for promoting apoptosis[37]. The simultaneous activation of these caspases strongly indicates that the Cs-RMIO nanocomposite induces apoptosis via the mitochondrial pathway. This result aligns with the findings of [38], which established mechanisms of nanoparticle-induced apoptosis, in which mitochondrial dysfunction triggers caspase activation**.** Activated caspase-9 cleaves and activates caspase-3, which is the main executor of cell disassembly. Similar outcomes observed by previous literature [39], indicating that chitosan-based nanocomposites significantly disrupt cells and elevate caspase-3 levels in HepG2 cells. They linked this effect to increased intracellular drug concentrations due to magnetic enhancement [40]. Fe_3O_4 nanoparticles induce apoptosis in cancer cells by increasing caspase-3 and caspase-9 expression, decreasing Bcl-2 expression, and inducing DNA damage[36]. The rise in caspase-9 and caspase-3 activities at 12 μg/mL in the current study highlights the effectiveness of Cs-RMIO NC as an inducer of apoptosis.

CONCLUSION

The current study demonstrates that Chitosan-Reduced Magnetic Iron Oxide nanocomposite exhibits strong anticancer activity against HepG2 cells via a well-coordinated, dose-dependent mechanism. The nanoparticles significantly reduced cell viability and induced morphological changes, suggesting cytotoxicity. Cs-RMIO nanocomposite generated excessive intracellular reactive oxygen species (ROS), resulting in oxidative stress and consequent damage to cellular components. The oxidative imbalance caused mitochondrial malfunction, as demonstrated by the loss of mitochondrial membrane potential, a key event in the onset of apoptosis. Furthermore, nuclear staining revealed substantial DNA damage, as evidenced by chromatin condensation and breakage. Disruption of cellular homeostasis caused increased lipid peroxidation and membrane damage, accompanied by an elevated but inadequate antioxidant response. Notably, the activation of caspase-9 and caspase-3 indicated that cell death happened via the intrinsic (mitochondrial) apoptotic pathway. The combination of cytotoxicity, biochemical, and fluorescence imaging data provides compelling evidence that the Cs-RMIO nanocomposite induces apoptosis via ROS-mediated mitochondrial signalling. Ultimately, these findings highlight that Chitosan Reduced Magnetic Iron Oxide Nanocomposite is a possible nanotherapeutic alternative for cancer treatment. Nonetheless, further in vivo studies and clinical trials are necessary to verify their safety, bioavailability, and effectiveness for potential biomedical uses.

REFERENCES

1. Ray, S.S. and J. Bandyopadhyay (2021): Nanotechnology-enabled biomedical engineering: current trends, future scopes, and perspectives. Nanotechnology Reviews, **10**(1): p. 728-743.
2. Ayyanaar, S., et al., (2020): ROS-responsive chitosan coated magnetic iron oxide nanoparticles as potential vehicles for targeted drug delivery in cancer therapy. International Journal of Nanomedicine, p. 3333-3346.
3. Zaiki, Y., A. Iskandar, and T.W. Wong, (2023): Functionalized chitosan for cancer nano drug delivery. Biotechnology Advances. **67**: p. 108200.
4. Sahdev, A.K., et al., (2022): Update on modified chitosan frameworks and their applications for food, wastewater, toxic heavy metals, dyes treatment and cancer drug delivery. Journal of Environmental Chemical Engineering, **10**(6): p. 108656.
5. Abhirami, S., et al., (2025): Eco-conscious synthesis of chitosan-reduced magnetic Iron oxide nanocomposite from crab Shell waste for photocatalytic degradation of textile dyes: Ecotoxicity insights. Journal of Water Process Engineering, **78**: p. 108651.
6. Wei, D. and W. Qian, (2008): Facile synthesis of Ag and Au nanoparticles utilizing chitosan as a mediator agent. Colloids and Surfaces B: Biointerfaces, **62**(1): p. 136-142.
7. Venkatesham, M., et al., (2014): A novel green one-step synthesis of silver nanoparticles using chitosan: catalytic activity and antimicrobial studies. Applied Nanoscience, **4**: p. 113-119.
8. Manikandan, A. and M. Sathiyabama (2015): Green synthesis of copper-chitosan nanoparticles and study of its antibacterial activity. J Nanomed Nanotechnol. **6**(1): p. 1.
9. Sachindra, N.M. and N. Bhaskar (2008): In vitro antioxidant activity of liquor from fermented shrimp biowaste. Bioresource technology, **99**(18): p. 9013-9016.
10. Vangijzegem, T., et al., (2023): Superparamagnetic iron oxide nanoparticles (SPION): from fundamentals to state-of-the-art innovative applications for cancer therapy. Pharmaceutics, **15**(1): p. 236.

11. Fahmy, H.M., et al., (2024): Enhanced biocompatibility by evaluating the cytotoxic and genotoxic effects of magnetic iron oxide nanoparticles and chitosan on Hepatocellular Carcinoma Cells (HCC). Cell Biochemistry and Biophysics, **82**(2): p. 1027-1042.
12. Rukhsar, M., et al., (2022): An overview of iron oxide (Fe3O4) nanoparticles: from synthetic strategies, characterization to antibacterial and anticancer applications. Crystals, **12**(12): p. 1809.
13. Salunkhe, A., et al., (2020): MRI guided magneto-chemotherapy with high-magnetic-moment iron oxide nanoparticles for cancer theranostics. ACS Applied Bio Materials, **3**(4): p. 2305-2313.
14. Bera, S., et al., (2014): Synthesis, characterization and cytotoxicity of europium incorporated ZnO–graphene nanocomposites on human MCF7 breast cancer cells. Rsc Advances, **4**(71): p. 37479-37490.
15. Patel, N.N., et al., (2024): Anticancer activity of surface functionalized magnetite (Fe3O4) nanoparticles—Effect of polymer coating. Emergent Materials, **7**(3): p. 1071-1080.
16. Dolati, M., et al., (2023); Biogenic copper oxide nanoparticles from Bacillus coagulans induced reactive oxygen species generation and apoptotic and anti-metastatic activities in breast cancer cells. Scientific Reports, **13**(1): p. 3256.
17. Tang, L., et al., (2024): Doxorubicin and iron-doped mesoporous silica nanoparticles for chemodynamic therapy and chemotherapy of breast cancer. New Journal of Chemistry, **48**(39): p. 17294-17309.
18. Xia, Y., et al., (2023): Microfluidic formulation of curcumin-loaded multiresponsive gelatin nanoparticles for anticancer therapy. ACS Biomaterials Science & Engineering. **9**(6): p. 3402-3413.
19. Chittasupho, C., et al., (2024): Clerodendrum chinense stem extract and nanoparticles: effects on proliferation, colony formation, apoptosis induction, cell cycle arrest, and mitochondrial membrane potential in human breast adenocarcinoma breast cancer cells. International Journal of Molecular Sciences, **25**(2): p. 978.
20. Doghish, A.S., et al., (2021): Graphene oxide and its nanocomposites with EDTA or chitosan induce apoptosis in MCF-7 human breast cancer. RSC advances, **11**(46): p. 29052-29064.
21. Gupta, P., et al., (2024): Unveiling the cytotoxic and anti-proliferative potential of green-synthesized silver nanoparticles mediated by Colletotrichum gloeosporioides. RSC advances, **14**(6): p. 4074-4088.
22. Ramalingam, V., S. Raja, and M. Harshavardhan (2020): In situ one-step synthesis of polymer-functionalized palladium nanoparticles: an efficient anticancer agent against breast cancer. Dalton Transactions, **49**(11): p. 3510-3518.
23. El-Mallul, A., et al., (2025): Advancements and future directions of iron oxide nanoparticles in cancer therapy. Contemporary Oncology/Współczesna Onkologia, **29**(1).
24. Mistral, J., et al., (2024): Chitosan-coated superparamagnetic Fe3O4 nanoparticles for magnetic resonance imaging, magnetic hyperthermia, and drug delivery. ACS Applied Nano Materials, **7**(7): p. 7097-7110.
25. Badry, M.D., et al., (2017): Synthesis, characterization, and in vitro anticancer evaluation of iron oxide/chitosan nanocomposites. Inorganic and Nano-Metal Chemistry, **47**(3): p. 405-411.
26. Liang, J., et al., (2011): Synthesis, characterization and cytotoxicity studies of chitosan-coated tea polyphenols nanoparticles. Colloids and Surfaces B: Biointerfaces, **82**(2): p. 297-301.
27. Lotfi, S., A. Bahari, and S. Mahjoub, (2019): In vitro biological evaluations of Fe3O4 compared with core–shell structures of chitosan-coated Fe3O4 and polyacrylic acid-coated Fe3O4 nanoparticles: S. Lotfi et al. Research on Chemical Intermediates, **45**(6): p. 3497-3512.
28. Prabaharan, M., (2015): Chitosan-based nanoparticles for tumor-targeted drug delivery. International journal of biological macromolecules, **72**: p. 1313-1322.
29. Qi, L., et al., (2004): Preparation and antibacterial activity of chitosan nanoparticles. Carbohydrate research, **339**(16): p. 2693-2700.
30. Gharu, C.P., (2022): Defense mechanism of natural antioxidants against free radicals. Central Asian Journal of Medical and Natural Science, **3**(5): p. 163-170.
31. Gholoobi, A., et al., (2017): Biopolymer-mediated synthesis of Fe3O4 nanoparticles and investigation of their in vitro cytotoxicity effects. Journal of Molecular Structure, **1141**: p. 594-599.
32. Liu, W., et al., (2020): Advanced biomimetic nanoreactor for specifically killing tumor cells through multi-enzyme cascade. Theranostics, **10**(14): p. 6245.
33. Gupta, A.K. and M. Gupta, (2005): Synthesis and surface engineering of iron oxide nanoparticles for biomedical applications. biomaterials, **26**(18): p. 3995-4021.
34. Magdolenova, Z., et al., (2015): Coating-dependent induction of cytotoxicity and genotoxicity of iron oxide nanoparticles. Nanotoxicology, **9**(sup1): p. 44-56.
35. Răcuciu, M., L. Barbu-Tudoran, and S. Oancea, (2025): Evaluation of phytotoxicity and genotoxicity of TMA-stabilized iron-oxide nanoparticle in corn (Zea mays) young plants. Scientific Reports, **15**(1): p. 18951.
36. Ranjbary, A.G., G.K. Saleh, and M. Azimi, (2021): Superparamagnetic Iron Oxide Nanoparticles Induce Apoptosis in HT-29 Cells by Increasing ROS and Damaging DNA.
37. Asselin, E., G.B. Mills, and B.K. Tsang, (2001): XIAP regulates Akt activity and caspase-3-dependent cleavage during cisplatin-induced apoptosis in human ovarian epithelial cancer cells. Cancer research, **61**(5): p. 1862-1868.
38. Lin, B., et al., (2017): Structural basis for alpha fetoprotein-mediated inhibition of caspase-3 activity in hepatocellular carcinoma cells. International Journal of Cancer, **141**(7): p. 1413-1421.

39. Elgohary, M.M., et al., (2018): Targeting sialic acid residues on lung cancer cells by inhalable boronic acid-decorated albumin nanocomposites for combined chemo/herbal therapy. Journal of Controlled Release, **285**: p. 230-243.
40. Elmore, S., (2007): Apoptosis: a review of programmed cell death. Toxicologic pathology, **35**(4): p. 495-516